BIODIVERSITAS
Volume 26, Number 12, December 2025
Pages: 6212-6223

ISSN: 1412-033X
E-ISSN: 2085-4722
DOI: 10.13057/biodiv/d261223

Environmental gradients of *Nypa fruticans* productivity and benthic macrofaunal assemblages in an acidic peat coastal ecosystem, Eastern Sumatra, Indonesia

HANAN AZ ZAHRA SYAFINA[1,♥], AGUS HARTOKO[2], PUJIONO WAHYU PURNOMO[2]

[1]Master Program of Aquatic Resources Management, Department of Aquatic Resources, Faculty of Fisheries and Marine Science, Universitas Diponegoro. Jl. Prof. Jacub Rais, Semarang 50275, Central Java, Indonesia. Tel./fax.: +62-76404447, ♥email: hazzahrasyafina@gmail.com

[2]Department of Aquatic Resources Management, Faculty of Fisheries and Marine Science, Universitas Diponegoro. Jl. Prof. Jacub Rais, Semarang 50275, Central Java, Indonesia

Manuscript received: 24 October 2025. Revision accepted: 7 December 2025.

Abstract. *Syafina HAZ, Hartoko A, Purnomo PW. 2025. Environmental gradients of* Nypa fruticans *productivity and benthic macrofaunal assemblages in an acidic peat coastal ecosystem, Eastern Sumatra, Indonesia. Biodiversitas 26: 6212-6223. Nypa fruticans* is a significant palm species found along tropical peat-fringed coasts; however, there is limited understanding of how its productivity and benthic fauna respond to hydrochemical gradients in acidic peat systems in this region. This study aimed to quantify the relationships of salinity and soil pH with *N. fruticans* aboveground biomass (AGB), carbon stocks, leaf chlorophyll, and benthic macrofauna along an estuarine–coastal gradient on an acidic peat coast in eastern Sumatra, Indonesia. We hypothesised that *Nypa* productivity and benthic richness and diversity would be highest in low-salinity, acidic estuarine plots and would decline towards saline, near-neutral coastal plots. We established 30 independent 10 × 10 m plots (10 per zone: estuarine, transitional, and coastal) and measured AGB (dry mass), carbon (C = 0.5 × AGB), leaf chlorophyll content, salinity, and soil pH. Benthic macrofauna were sampled using three 25 × 25 cm quadrats per plot, and diversity indices were calculated from quadrat and plot-level abundances. Differences among zones and their associations with environmental variables were assessed using ANOVA, non-parametric tests, correlation analysis, and PCA. AGB decreased from 45.9 ± 4.2 t ha^{-1} in the estuarine zone to 3.1 ± 1.7 t ha^{-1} and 1.1 ± 0.5 t ha^{-1} in the transitional and coastal zones ($F_{2,27}$ = 41.52, $p < 0.001$), with proportional reductions in the carbon stocks. Chlorophyll content was correlated with AGB ($r = 0.84$, $p < 0.001$), supporting its use as a measure of vigour. Benthic diversity (Shannon H′) declined from 1.450 in estuarine plots to 1.073 in coastal plots, and total benthic abundance decreased seaward, parallel to the declining *Nypa* productivity. Over this gradient, salinity increased from 0-1.4‰ to 9-10‰, and soil pH shifted from acidic (~2.35) to near-neutral (~7.0). Biotic variables were negatively associated with the salinity–pH axis in the PCA, indicating that hydrochemical gradients jointly structured the vegetation and benthos. This first gradient-based study of Indonesia's acidic peat coasts quantifies *Nypa* productivity and benthic macrofauna along a salinity–pH gradient, providing a baseline for future multi-season investigations.

Keywords: Acidic peat coast, benthic macrofauna, biomass, *Nypa fruticans*, productivity

INTRODUCTION

Tropical peat–coastal systems function as dynamic interfaces between terrestrial and marine environments, where the interaction of freshwater discharge, tidal inundation, and acidic organic soils influences both the vegetation and faunal communities. Along the eastern coast of Sumatra, extensive peat deposits converge with macrotidal estuaries, creating pronounced gradients in salinity, acidity, and sediment characteristics (Hapsari et al. 2022). These gradients are pivotal in affecting carbon storage, shoreline stability, and habitat provisioning, while simultaneously subjecting coastal ecosystems to the challenges of rising sea levels and salinity intrusions. In such contexts, even minor alterations in hydrology or water chemistry can impact plant productivity and faunal assemblages, with significant implications for blue carbon stocks and local livelihoods, as emphasised in recent reviews of mangrove and coastal peat management (Arifanti et al. 2022; Adame et al. 2024). Building on previous research conducted at Pangkal Babu, which quantified morphometric gradients and clump density of *Nypa fruticans* Wurmb along the same estuarine–coastal transect (Syafina et al. 2025), this study extends the investigation by estimating the aboveground biomass, carbon stocks, and leaf chlorophyll. We conducted a comprehensive analysis of these vegetation metrics in conjunction with benthic macrofaunal assemblages and hydrochemical gradients.

Within these peat-fringed estuaries, the nipa palm (*N. fruticans*) represents a structurally and socioeconomically significant mangrove species. *Nypa* stands contribute to bank stabilisation, wave attenuation, and sediment trapping, whereas litterfall and root exudates enhance nutrient and carbon cycling in adjacent mudflats and channels (Afonso et al. 2021; Hatje et al. 2023). The substantial frond biomass and dense root mats provide materials for construction and small-scale fisheries, thereby directly linking *Nypa* productivity to the livelihoods of coastal communities in Indonesia (Abidin et al. 2021; Rumondang et al. 2024). Recent genomic and eco-physiological research indicates that *N. fruticans* can endure a broad range of salinities and flooded conditions, although its productivity may be influenced by the combined

effects of salinity, acidity, and sediment properties (Xu et al. 2021; Yoshikai et al. 2022; Wu et al. 2024). Nonetheless, quantitative assessments of *Nypa* biomass, carbon stocks, and physiological traits across environmental gradients in acidic peat settings are limited.

Benthic macrofauna, including mudskippers (*Periophthalmus* spp.) and fiddler crabs (*Uca* spp.), play crucial functional roles on *Nypa*-dominated shorelines of mangrove forests. Through activities such as burrowing, grazing, and bioturbation, these organisms enhance sediment aeration, facilitate the decomposition of organic matter, and promote nutrient recycling, thereby influencing secondary production and food web structures (Coppock et al. 2021; Lam-Gordillo et al. 2021; Hui et al. 2024; Qureshi and Saher 2024). Benthic assemblages are highly responsive to factors such as salinity, sediment grain size, and organic matter availability, and have been used as indicators of environmental change in estuarine and mangrove systems (Meijer et al. 2021; Broman et al. 2022; Lobo et al. 2024). However, in peat-influenced estuaries, the combined responses of dominant benthic taxa and *Nypa* stands to measured hydrochemical gradients remain insufficiently documented, thereby limiting our ability to link vegetation structure, biodiversity, and ecosystem function.

To our knowledge, limited research has simultaneously quantified *Nypa* productivity—encompassing biomass, carbon, and chlorophyll—and the structure of benthic macrofauna along salinity–pH gradients on the acidic peat coasts of Indonesia. Most existing studies either focus on mangrove biomass and blue carbon stocks without incorporating faunal data or examine benthic communities without detailed vegetation metrics. This study addresses this gap by employing a structured sampling design across an estuarine–transitional–coastal gradient in Pangkal Babu, Jambi (Eastern Sumatra). We delineated three habitat zones characterized by local salinity (0-10‰) and soil pH (2.35-7.0) and measured *Nypa* aboveground biomass, carbon, leaf chlorophyll, benthic macrofauna, salinity, and soil pH in each zone. Specifically, we posed the following questions: (i) How do *Nypa* biomass, carbon, and chlorophyll vary along the salinity–pH gradient? (ii) How do benthic richness, abundance, and diversity covary with *Nypa* productivity? (iii) Does multivariate ordination reveal a dominant environmental axis that structures vegetation and benthos? We hypothesised that both *Nypa* productivity and benthic diversity would decline with increasing salinity and pH, with benthic assemblages covarying positively with *Nypa* biomass and chlorophyll.

MATERIALS AND METHODS

Time and sampling site determination

Field sampling was conducted from May to June 2025 using purposive sampling during the late wet season in Pangkal Babu, Eastern Sumatra, Indonesia (Figure 1). Owing to logistical constraints, the data represent spatial variations within a single hydrological period. Three ecological zones were identified: Zone 1 (estuarine) near the river mouth, Zone 2 (transitional) characterized by brackish water, and Zone 3 (coastal) affected by seawater intrusion (Table 1). These zones were delineated based on salinity and soil pH measurements, ranging from oligohaline, acidic peat to mesohaline, near-neutral peat-mud mixtures near the coast (Table 7). Plots were spaced 150-200 m apart to minimize spatial autocorrelation and to ensure distinct *Nypa* stands.

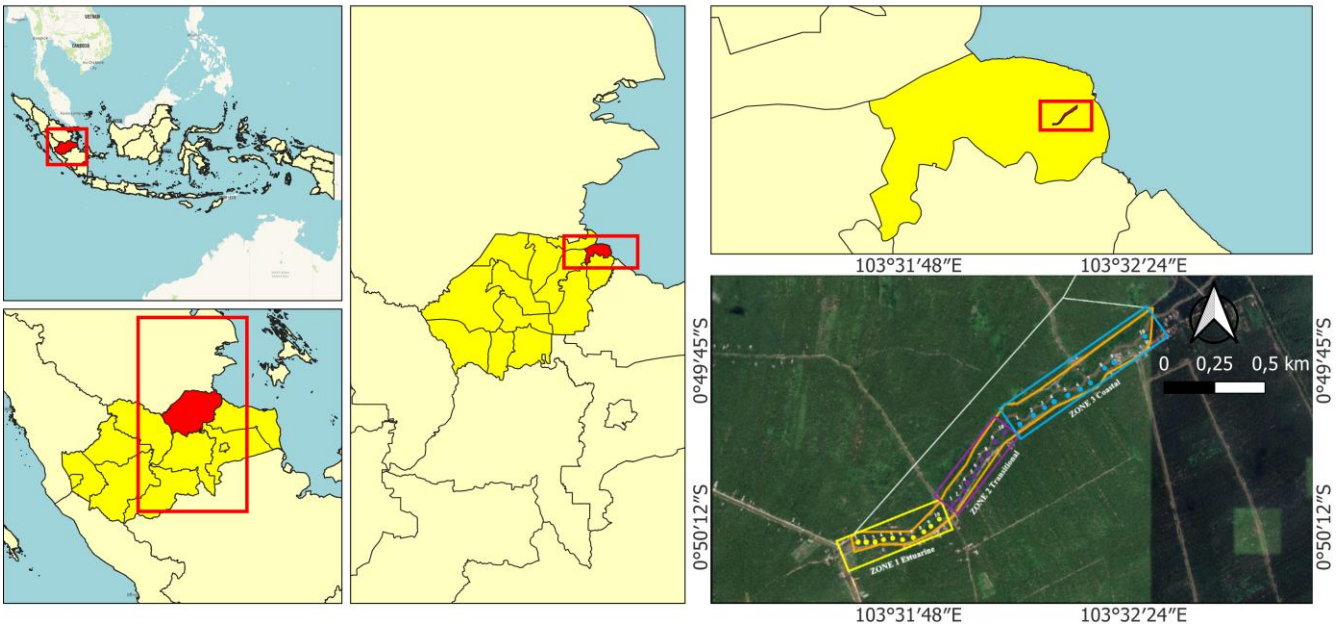

Figure 1. Study area and sampling stations in Pangkal Babu, Eastern Sumatra, Indonesia. Zones: estuarine (Z1), transitional (Z2), coastal (Z3)

Table 1. Description of the locations and GPS coordinates for each sampling site

Location/station	GPS coordinate	Description
Pangkal Babu, Tungkal I Village, Tungkal Ilir Sub-district, Tanjung Jabung Barat District, Jambi Province, Indonesia		The acidic peat coastal landscape experiences tidal flushing and freshwater inputs, with semidiurnal tides ranging from 1.6 to 2.1 m affecting hydrology, vegetation, and salinity
Upstream	103°31′41.65″E 0°50′14.05″S	*Nypa fruticans* stands grown on low-salinity acidic peat (pH 2.35). The area receives freshwater during high tides with minimal human activity limited to fishing shelters. Significant accumulation of litter and detritus was observed
Mid-estuary	103°32′0.98″E 0°50′0.47″S	Mixed vegetation of *Nypa, Rhizophora,* and *Avicennia* grows on peaty mud with salinity of 1.5-2.8 ‰. The ecosystem experiences alternating freshwater and saline tides. The adjacent land contains coconut and areca nut plantations
Downstream	103°32′16.11″E 0°49′48.49″S	The vegetation consisted of sparse *Nypa fruticans* and halophytic shrubs on peat mud substrates. The area has mesohaline of 9–10 ‰ and experienced marine influence during spring tides, bordered by mudflats and mangrove fringes with limited vegetation

Figure 2. Plot layout along the gradient with systematic 150-200 m spacing (n = 30 plots) (Captured using a DJI Phantom 4 Pro UAV drone)

A purposive transect design was employed to capture estuarine–transitional–coastal gradients, with 30 plots (10 × 10 m) established along the shore (Figure 2). The estimates reflect gradient-focused upper bounds due to non-random sampling. Environmental parameters were measured in situ, and soil and vegetation samples were analyzed at Universitas Jambi. The semidiurnal tidal regime (1.6-2.1 m) influenced the sediment conditions. Vegetation and benthic samples were collected within ± 2 h of low tide.

Vegetation and environmental data collection

Data were systematically collected at each of the 30 sampling stations, with 10 stations allocated per ecological zone, to investigate the morphometric and environmental characteristics of *N. fruticans* and its surrounding habitats. Sampling plots, each measuring 10 × 10 m, were established within each zone, with each plot serving as an independent replicate of the study. The number of stations per zone was determined based on prior coastal vegetation studies (Alongi 2020; Basyuni et al. 2022) and field accessibility, ensuring representative coverage of the hydrological and salinity gradients while maintaining sufficient replication for statistical analysis. Within each plot, *N. fruticans* clumps were selected for morphometric measurements, including frond number (Σf), mean frond length (m), and frond basal diameter (cm). The fresh weight of each frond (Wf, kg)

was measured using a portable digital scale with a precision of ± 0.01 kg. Within each plot, three 25 × 25 cm (0.0625 m²) benthic quadrats were randomly positioned to mitigate placement bias. Each plot was treated as an independent replicate for all subsequent statistical analyses. The morphometric and clump-density data for *N. fruticans* used in this study to derive biomass were derived from the dataset initially described by Syafina et al. (2025), where they were analysed exclusively in terms of structural zonation. In the current study, we reanalysed these measurements to estimate the aboveground biomass, carbon stocks, and their relationships with benthic macrofauna.

To ascertain the dry weight ratio, subsamples of representative fronds were oven-dried at 70°C until a constant weight was achieved. Environmental parameters were assessed in situ at each sampling site. Salinity (‰), soil pH, temperature, and tidal amplitude were measured in situ using a handheld refractometer, portable pH meter, field thermometer, and staff gauge, respectively. All instruments were calibrated daily following the manufacturer's instructions, and salinity and pH values represent the mean of three readings per plot; results are reported as mean ± SD.

Due to logistical constraints, we did not assess the sediment organic matter content, N–P–K concentrations, or grain size distribution. Instead, sediment conditions were characterized in situ using qualitative substrate categories (silty clay, peaty mud, and peat–mud mix) and by measuring the salinity and pH. The absence of detailed sediment chemistry and temporal replication is acknowledged as a limitation and addressed in the discussion and conclusion sections.

Biomass and carbon estimation

The estimation of aboveground biomass (AGB; dry mass) per clump was conducted using the formula:

$$AGB\_clump = \Sigma f \times Wf\_fresh \times DW\_ratio.$$

In this equation, Σf represents the number of fronds per clump, Wf_fresh denotes the mean fresh weight (kg) of the fronds, and DW_ratio is the dry-to-fresh mass ratio, which was determined by oven-drying representative frond subsamples at 70 °C until a constant mass was achieved (n = 10). The area-based AGB (t ha^{-1}) was calculated by multiplying the mean AGB_clump by the clump density (clumps ha^{-1}) obtained from 10 × 10 m plots and then scaling the result to 1 ha.

The carbon stock (t C ha^{-1}) was determined using the formula C = 0.50 × AGB (dry weight) (Brown 1997; Murdiyarso et al. 2009. All biomass values presented pertain to aboveground biomass (AGB) stocks, quantified as t ha^{-1} (dry mass). Carbon stock was quantified as t C ha^{-1}. As sampling was conducted only once per station, this study did not provide estimates of annual production rates (t ha^{-1} yr^{-1}).

For each zone, the dry-to-fresh mass ratio (DW_ratio) was estimated from 10 representative fronds (n = 10 per zone) that were oven-dried to a constant weight. DW_ratio values were summarized as mean ± Standard Deviation (SD) and applied to plot-level fresh mass measurements to obtain clump-level AGB. Plot-level AGB (t ha^{-1}) and carbon stocks (t C ha^{-1}) were then averaged within each zone, with SD and standard errors reflecting the variability among plots. This approach propagates uncertainty in both clump density and biomass per clump into the zone-level estimates reported in Table 3.

Chlorophyll measurement

Leaflet samples were immediately stored in dark containers on ice and transported to the laboratory. Chlorophyll was extracted in 80% acetone and measured using a UV–Vis spectrophotometer (Orion AquaMate 8100) at 652 nm, following MacKinney (1941) and Arnon (1949):

$$\mathbf{Chl_{total(mg\ L^{-1})}} = \frac{\mathbf{A_{652} \times 1000 \times DF}}{\mathbf{34.5 \times \mathit{l}}}$$

Where, A_{652}: Absorbance value (At 652 nm, chlorophyll a and b intersect), DF: Dilution Factor, *l*: Path length (cm), 34.5: Combined specific absorption coefficient for chlorophyll a + b in 80% acetone at 652 nm.

Benthic fauna sampling

In each plot, three quadrats measuring 25 × 25 cm were randomly positioned within the 10 × 10 m plot and excavated to a depth of 10 cm, resulting in a total sample size of 90 quadrats. The collected samples were washed over a 0.5-mm mesh and preserved in 70% ethanol. Taxonomic identification was conducted using Carpenter and Niem (1998) and FAO (1999) as references, with ambiguous specimens assigned to the most consistent taxonomic levels. A 10% subset of the specimens was re-evaluated by a second taxonomist for verification of the results. For each plot, individuals from the three quadrats were aggregated to obtain plot-level counts (individuals per 10 × 10 m plot; 100 m²), which were subsequently averaged within each zone to compute the diversity indices. The sampling protocol specifically targeted conspicuous, surface-active macrofauna such as mudskippers and crabs, rather than the entire infaunal community. Consequently, smaller-bodied and deep-burrowing taxa, including many polychaetes and bivalves, were likely to be under-represented.

The abundance of each taxon (Ni) and total individuals (N) were recorded to calculate the biodiversity indices as follows:

Shannon–Wiener Diversity Index (H')

$$H' = -\sum \left(\frac{ni}{N}\right) ln \left(\frac{ni}{N}\right)$$

A diversity index was used to evaluate the degree of benthic diversity within a population. This index is based on the Shannon-Wiener formula (Shannon 1948; Yazdian et al. 2014; Magurran 2021).

Where: H': Shannon-Wiener Diversity Index, ni: Number of individuals/species, N: Total number of individuals

Simpson Dominance Index (C)

The dominance index is used to assess the extent to which a particular organism dominates other organisms within an ecosystem. This index was quantified using Simpson's Index of Dominance (Simpson 1949; Custodio et al. 2018) as follows:

$$C = \sum \left(\frac{ni}{N}\right)^2$$

Where: C: Dominance Index, ni: Number of individuals of each type, N: Total number of Individuals

Evenness Index (E)

The Evenness Index quantifies the distribution of individuals across the species identified in this study. This index was determined using Pielou's Index (Pielou 1966; Custodio et al. 2018; Magurran 2021) as follows:

$$E = \frac{H'}{LnS}$$

Where: E: Evenness Index, H': Shannon-Wiener Diversity Index, LnS: Natural log of the total number of species

Data analysis

We evaluated normality and homogeneity of variances using the Shapiro–Wilk and Levene tests. In instances where assumptions were violated, we applied a log10(x + 1) transformation to the data or employed Kruskal–Wallis tests with Dunn–Holm post-hoc comparisons. Differences among zones were assessed using one-way ANOVA, followed by Tukey's HSD or Kruskal–Wallis tests, as appropriate. Pearson or Spearman correlations were utilized depending on the data distributions. Principal Component Analysis (PCA) was conducted on centred and scaled variables, including salinity, pH, aboveground biomass, chlorophyll, Shannon H′, species richness, and total abundance; carbon (0.5 × AGB) was excluded from the PCA to prevent redundancy. PCA was used as an exploratory ordination, and the sample-to-variable ratio (30 plots and seven variables) satisfied the common guidelines for multivariate analyses. All analyses were performed using SPSS v25 with a significance level of $\alpha = 0.05$.

RESULTS AND DISCUSSION

***Nypa fruticans* productivity**

The aboveground biomass (AGB), carbon stocks, and leaf chlorophyll content of *N. fruticans* showed significant variation across different zones. A one-way ANOVA conducted at the plot level revealed a substantial zone effect on AGB ($F_{2,27} = 41.52$, $P < 0.001$; Table 3). The mean AGB was highest in the estuarine plots and considerably lower in the transitional and coastal plots, indicating an approximate 95% reduction in AGB from the estuary to the coast. These variations were associated with shorter fronds, fewer fronds per clump, and decreased clump density downstream (Table 2; Figure 4).

Leaf chlorophyll concentration was positively correlated with both AGB and carbon stocks ($r = 0.84$ and 0.87, respectively; $p < 0.01$; Tables 3 and 4), and chlorophyll accounted for approximately 70% of the variation in carbon among plots (polynomial regression, $R^2 \approx 0.70$). The mean chlorophyll content was comparable in the estuarine and transitional plots and was slightly lower at the coast (Table 4).

Table 2. Morphometric characteristics of *Nypa fruticans* by zone. Values are mean ± SD

Parameter	Zone 1 estuarine (n = 10)	Zone 2 transitional (n = 10)	Zone 3 coastal (n = 10)
Frond height (m)	7.32 ± 0.82	6.11 ± 0.49	3.57 ± 0.56
Leaves in frond (unit)	122.3 ± 4.4	109.6 ± 9.7	90.4 ± 10.7
Fronds in clump (unit)	12.2 ± 1.8	7.8 ± 0.6	6.4 ± 1.2
Clump density (clumps ha^{-1})	510	126	100

Table 3. AGB and carbon stocks by zone (t ha^{-1} and t C ha^{-1}; mean ± SD; n = 10). Carbon computed as 0.5 × AGB

Ecological zone	Mean frond weight Wf (kg)	Mean frond number Σf (unit)	Biomass (t ha^{-1})	Carbon (t C ha^{-1})
Zone 1 – estuarine	7.60 ± 1.41	12.2 ± 1.6	45.9 ± 4.2	23.0 ± 2.1
Zone 2 – transitional	3.47 ± 0.49	7.8 ± 0.6	3.1 ± 1.7	1.6 ± 0.9
Zone 3 – coastal	2.45 ± 0.62	6.4 ± 1.2	1.1 ± 0.5	0.6 ± 0.3

Table 4. Total chlorophyll concentration and estimated chlorophyll content in *Nypa fruticans*

Zone	Leaf chlorophyll (mg L^{-1})	Leaves in frond	Fronds in clump
Zone 1 – estuarine	2.175	122	12
Zone 2 – transitional	2.105	110	8
Zone 3 – coastal	1.915	90	6
Total	6.195	322	26
Mean ± SD	2.065 ± 0.13	107 ± 16	9 ± 3

Table 5. Benthic fauna associated with *Nypa fruticans* stands across various ecological zones

Taxon	Family	Zone 1 (estuarine)	Zone 2 (transitional)	Zone 3 (coastal)	Mean abundance (± SD, individuals plot^{-1}; 100 m²)	Abundance class*	Ecological role
Periophthalmus gracilis (Eggert, 1935)	Gobiidae	62 ± 8	45 ± 6	15 ± 4	41 ± 10	+++	Bio-indicator of muddy substrate stability
Periophthalmodon schlosseri (Pallas, 1770)	Gobiidae	48 ± 7	32 ± 5	10 ± 3	30 ± 9	++	Sediment aeration and surface activity
Uca sp. (fiddler crab)	Ocypodidae	40 ± 5	27 ± 4	9 ± 2	25 ± 8	++	Bioturbation and organic-matter recycling
Parathelphusa spp.	Gecarcinucidae	18 ± 4	8 ± 3	–	9 ± 4	+	Sediment bioturbation and nutrient cycling
Thalamita crenata (Rüppell, 1830)	Portunidae	10 ± 3	5 ± 2	–	5 ± 3	+	Detritivore and decomposer of organic debris

Note: Abundance classification: (+++): abundant, (++): moderate, (+): rare, (−): absent. Values are presented as mean ± Standard Deviation (SD) of plot-level counts (n = 10 plots per zone). For each plot, individuals from three 25 × 25 cm quadrats were aggregated, and abundance was expressed as individuals per 10 × 10 m plot (100 m²). Diversity indices were calculated from plot-level abundances and averaged within each zone

Table 6. Benthic diversity metrics by zone, derived from the mean abundances at the plot level, are presented in Table 5 (N = total individuals per 10 × 10 m plot)

Zone	S	N (individuals plot^{-1}; 100 m²)	Shannon–Wiener Diversity Index (H′) (log natural)	Simpson dominance (C)	Simpson diversity (1−C)	Evenness (E)
Estuarine (Z1)	5	178	1.450	0.258	0.742	0.901
Transitional (Z2)	5	117	1.379	0.282	0.718	0.857
Coastal (Z3)	3	34	1.073	0.351	0.649	0.977

Benthic macrofaunal assemblages

Five prominent benthic macrofaunal taxa were identified along the gradient: *Periophthalmus gracilis* Eggert, 1935, *P. schlosseri*, *Uca* sp., *Parathelphusa* spp., and *Thalamita crenata* Rüppell, 1830 (Table 5). Both mean plot-level abundances (individuals per 10 × 10 m plot; 100 m²) and taxon richness declined from the estuarine to the coastal zones, whereas evenness increased. The Shannon (H′) and Simpson diversity (1−C) indices were highest in the estuarine plots and lowest in the coastal plots (Table 6), with plot-level H′ showing significant variation among zones ($F_{2,27} = 23.46$, $p < 0.001$). *Parathelphusa* spp. and *T. crenata* were absent from the coastal plots, whereas *P. gracilis*, *P. schlosseri*, and *Uca* sp. were present across all three zones, albeit with reduced abundance in the seaward direction (Table 5; Figure 3). Gastropods were occasionally observed on the exposed prop roots of adjacent *Rhizophora* and *Avicennia* at the fringes of our plots, but none were found within the 25 × 25 cm quadrats placed under dense *Nypa* stands; consequently, no gastropod taxa are listed in Table 5.

Environmental parameters

Salinity and soil pH demonstrated distinct spatial gradients across the three zones (Table 7). Estuarine plots were characterized by oligohaline conditions and strongly acidic peat, with salinity ranging from 0.0 to 1.4‰ and soil pH of 2.35. In contrast, transitional plots exhibited slightly elevated salinity levels (1.5-2.8‰) and moderately acidic peaty mud with a pH of 4.3. Coastal plots were subject to mesohaline conditions, with salinity between 9.0 and 10.0‰ and near-neutral peat–mud mixtures with a pH of 7.0. Temperature variations among the zones were minimal, ranging from 28.3 ± 0.4°C in coastal plots to 29.1 ± 0.5°C in estuarine plots, as detailed in Table 7. The substrate types also transitioned along the gradient, from silty clay upstream to peaty mud in the mid-estuary and peat–mud mixtures near the coast, accompanied by shifts in the dominant vegetation composition.

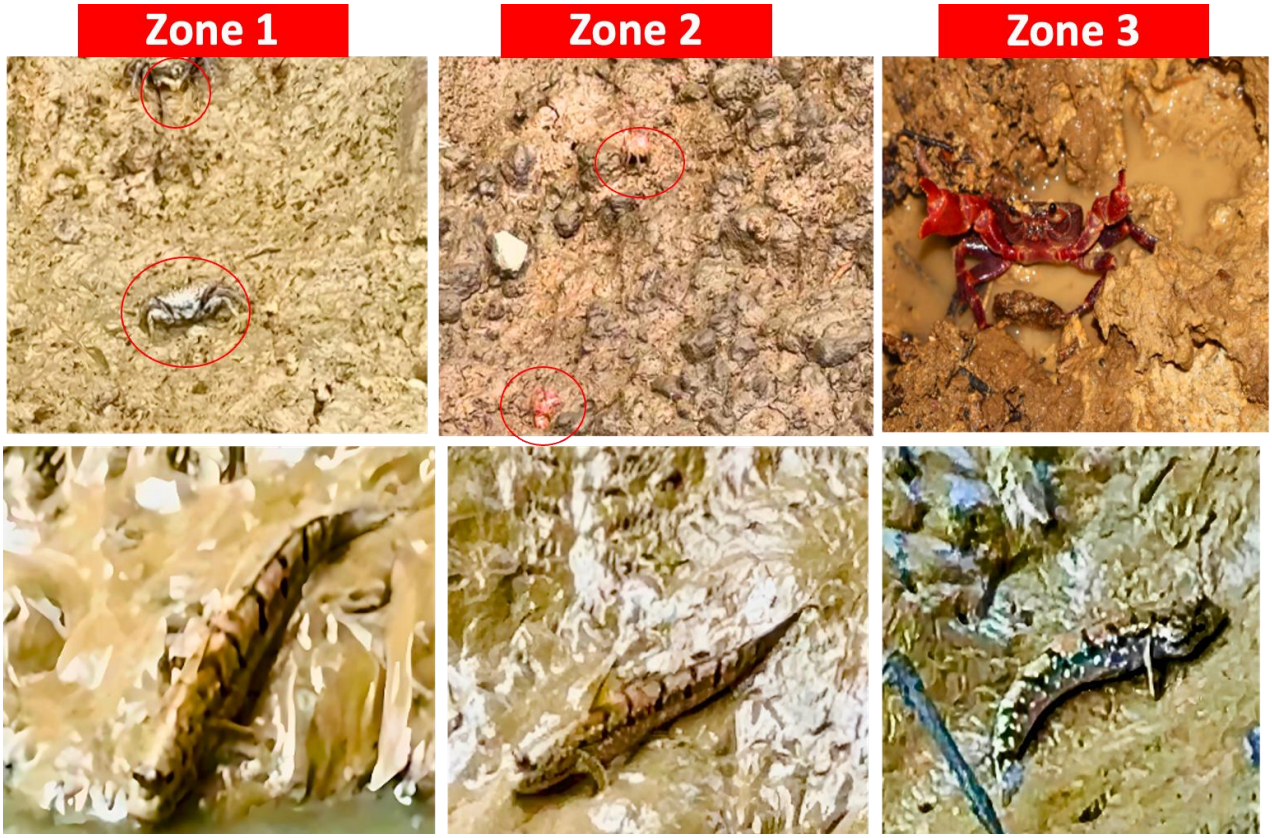

Figure 3. Zonation of surface-active benthic macrofauna associated with *Nypa fruticans* along the estuarine–coastal gradient in Pangkal Babu, Jambi, Indonesia. The upper panels depict crustaceans: small *Uca* spp. in estuarine mudflats, pinkish fiddler crab *Gelasimus vocans* in transitional zones, and larger reddish crabs in coastal areas. The lower panels display mudskippers (*Periophthalmus gracilis* and *Periophthalmodon schlosseri*), highlighting the shift in abundance and body size from low-salinity estuaries to high-salinity coastal zones, reflecting physiological adaptation to environmental stress

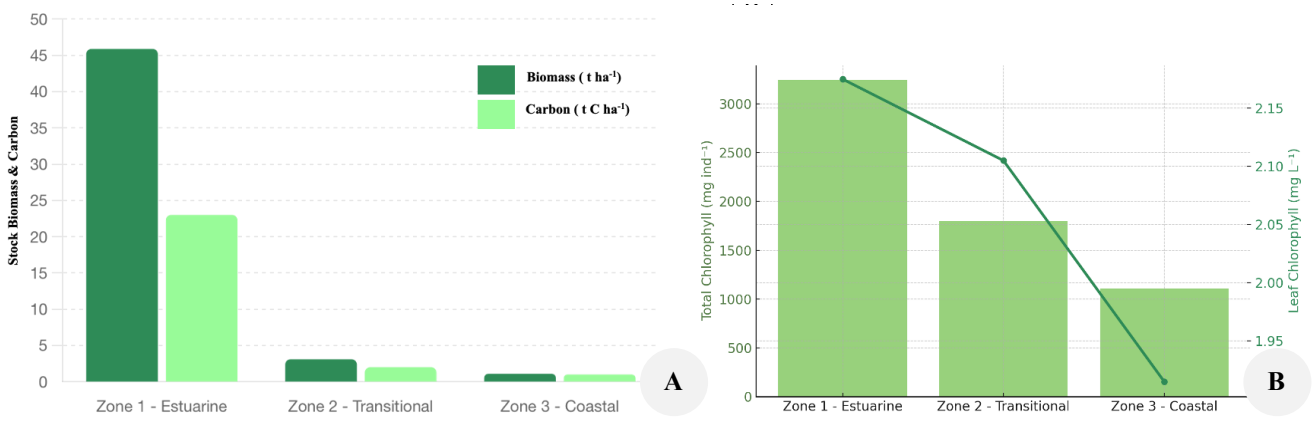

Figure 4. *Nypa* productivity in each zone. A. AGB (t ha^{-1}) and carbon (t C ha^{-1}) as mean ± SD with Tukey HSD, α= 0.05. B. Leaf chlorophyll (mg L^{-1}); points are plot means

Multivariate and bivariate relationships among vegetation, benthos, and hydrochemical gradients

Principal component analysis (PCA) of salinity, pH, aboveground biomass (AGB), chlorophyll, Shannon H′, species richness, and total abundance accounted for 83.6% of the variance within the first two components (PC1:59.2%, PC2:24.4%; Figure 5). PC1 predominantly represented the salinity–pH gradient, along which AGB, chlorophyll, and benthic diversity and abundance exhibited negative correlations. Estuarine, transitional, and coastal plots were distinctly separated along PC1, indicating variations in hydrochemical conditions and corresponding biotic responses.

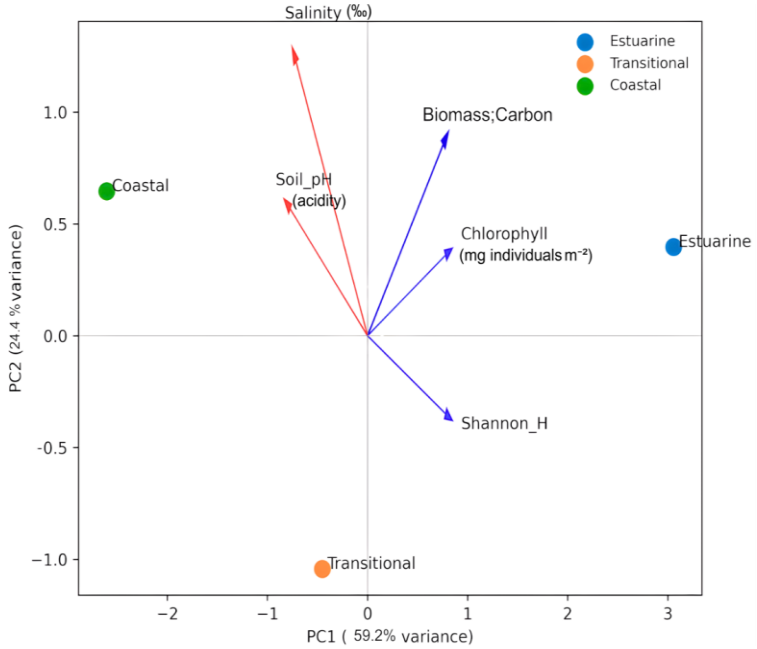

Figure 5. PCA ordination of environmental gradients and biotic variables across *Nypa fruticans* ecological zones. Principal component analysis revealed relationships between salinity, pH, and biotic indicators in the estuarine zones. Axis X (PC1, 59.2% of the variance) represented the salinity–pH gradient, whereas Axis Y (PC2, 24.4%) was correlated with residual biotic structure. Biotic variables showed negative loadings on PC1, indicating reduced productivity at higher salinity

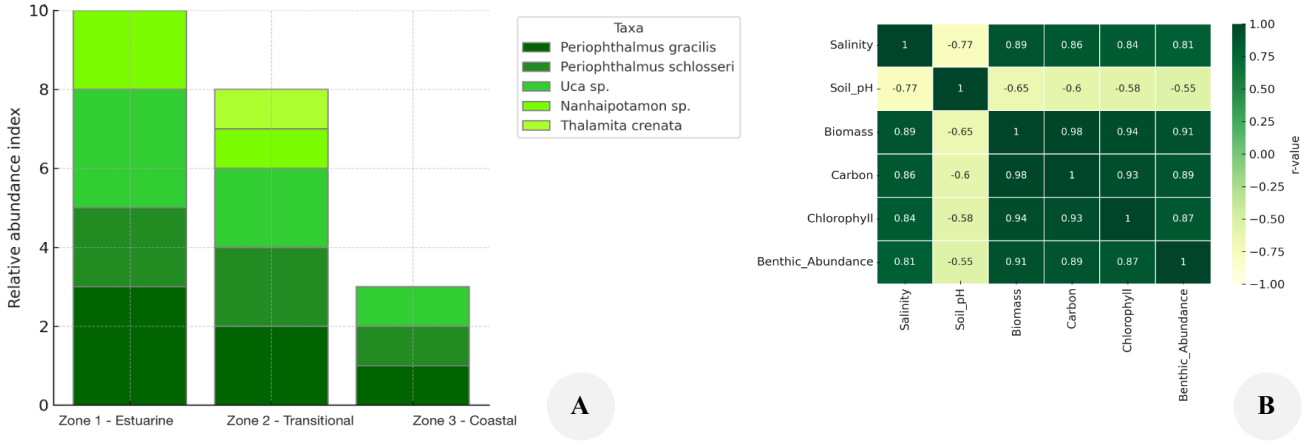

Figure 6. Benthic macrofaunal assemblages and ecological correlation patterns in *Nypa fruticans* ecosystems. A. Composition of benthic macrofauna associated with *N. fruticans*; relative abundance of *Periophthalmus gracilis*, *Periophthalmodon schlosseri*, *Uca* sp., *Parathelphusa* spp., and *Thalamita crenata* across the ecological zones. B. Correlations among environmental factors, *Nypa* productivity, and macrofaunal diversity. The heatmap shows strong positive correlations among biomass, carbon, chlorophyll, and macrofaunal indices and negative correlations with soil pH

Table 7. Environmental characteristics of *Nypa fruticans* habitats across three ecological zones in Pangkal Babu, Eastern Sumatra, Indonesia

Parameter	Zone 1 (estuarine)	Zone 2 (transitional)	Zone 3 (coastal)
Salinity (‰)	0.0-1.4	1.5-2.8	9.0-10.0
Soil pH (acidity)	2.35	4.3	7.0
Temperature (°C)	29.1 ± 0.5	28.7 ± 0.6	28.3 ± 0.4
Substrate type	Silty clay	Peaty mud	Peat–mud mix
Dominant vegetation	*Nypa fruticans*	*Nypa fruticans*, *Rhizophora mucronata*, *Avicennia marina*	*Nypa fruticans*, *Rhizophora mucronata, Avicennia marina*
Distance from shoreline (km)	3.0	2.5	1.5

Note: The pH values of the soil pertain to peat pore-water measured in 1:2 soil-water slurries, thereby reflecting substrate acidity rather than the pH of the water column

Discussion

Our findings indicate that along the peat-fringed estuarine–coastal gradient of Pangkal Babu, both the productivity of *N. fruticans* and benthic macrofauna diminish seaward, concomitant with increasing salinity and a transition from strongly acidic to near-neutral peat–mud substrate. Aboveground biomass and carbon stocks exhibited a reduction of approximately 95% from estuarine to coastal plots, with leaf chlorophyll showing a similar decline. In contrast, benthic richness, Shannon diversity, and total abundance were most pronounced in the estuarine plots and least at the coast (Tables 3-6). These concurrent declining trends are evident in the PCA, where AGB, chlorophyll, H′, richness, and abundance load negatively on the salinity–pH axis, and in the strong positive correlations between *Nypa* productivity metrics and benthic diversity ($r > 0.75$, $p < 0.01$), and negative correlations with salinity and pH (Figures 5 and 6). We regard the PCA as an exploratory representation of the primary salinity–pH gradient rather than as a predictive or mechanistic model because of the limited number of environmental variables measured in this study. Collectively, these results suggest that the observed hydrochemical gradient exerts a uniform influence on vegetation and benthos, with *Nypa* productivity and benthic assemblages being closely linked within the acidic peat coastal system.

Given the correlative and single-season design, these relationships cannot be definitively interpreted as causal; however, they align with a bottom-up framework in which hydrological and chemical conditions influence *Nypa* productivity, which subsequently affects benthic diversity through habitat structure and organic matter supply. The estuarine plots, characterized by low salinity and strongly acidic peat, supported the tallest canopies, highest clump densities, and greatest AGB and carbon stocks, as well as the most diverse and abundant macrofaunal assemblages. In contrast, the more saline and near-neutral coastal plots exhibited sparse *Nypa* stands with simplified benthic communities.

The hydrological conditions at Pangkal Babu, characterised by the interaction between macrotidal flooding and freshwater discharge from peatlands, significantly influence salinity and inundation patterns, affecting *Nypa* roots and benthic fauna (Table 7). This interaction also determines the residence time of dissolved organic carbon and nutrients in the estuary. In the upper estuary, frequent freshwater flushing maintains low pore water salinity and exports peat-derived organic matter, supporting high biomass, chlorophyll, and benthic richness. Conversely, coastal plots with limited freshwater inputs are inundated for extended periods with saline water, increasing osmotic stress and constraining the delivery of organic and nutrient subsidies, which likely contributes to the observed reductions in *Nypa* productivity and benthic diversity. These patterns are consistent with long-term studies, indicating that hydrological connectivity and flooding regimes strongly regulate productivity in coastal wetlands and mangroves (Reed et al. 2022; Vázquez-Rosas-Landa et al. 2025).

Within this hydrological context, the shift in soil pH from ~2.35 in the estuarine peat to ~7.0 in coastal peat–mud mixtures suggests concurrent changes in ionic composition, nutrient availability, and metal solubility (Table 7). Experimental and theoretical work indicates that salinity can limit mangrove canopy height and productivity by reducing hydraulic conductivity and carbon assimilation (Perri et al. 2023). Our data align with this expectation: the highest *Nypa* biomass and chlorophyll occurred where salinity was lowest, and both metrics declined with rising salinity and pH. Although we did not measure plant water status, nutrient concentrations, or gas exchange, the joint negative associations of *Nypa* productivity and benthic diversity with the salinity–pH axis support the interpretation that hydrochemical conditions constitute a primary environmental filter along the gradient.

The strong positive correlations between aboveground biomass and Shannon diversity (H′) suggest that plots characterized by structurally complex and productive *Nypa* stands tend to support richer and more abundant macrofaunal assemblages (Figure 6). In estuarine plots with high biomass, the presence of dense root mats and abundant litterfall enhances habitat complexity, detrital input, and the formation of oxygenated micro-niches, collectively favoring detritivores and burrowing organisms. *Periophthalmus gracilis*, *P. schlosseri*, and *Uca* sp. were most prevalent in these environments, consistent with their roles as surface-active bioturbators that aerate sediments, process organic matter, and regulate invertebrate populations (Cannicci et al. 2021; Meijer et al. 2021; Hui et al. 2024; Qureshi and Saher 2024). Conversely, the decline and eventual absence of *Parathelphusa* spp. and *T. crenata* in coastal plots coincided with the transition to more compact peat–mud substrates and increased salinity (Tables 5, 6 and 7). Larger burrowing crabs may be less capable of maintaining complex burrow systems in compact saline sediments, potentially reducing burrow heterogeneity and niche availability for smaller invertebrates. Changes in pH and ionic composition are also anticipated to influence redox conditions and nutrient cycling, further affecting the habitat quality. Similar associations between salinity, sediment geochemistry, and macrofaunal diversity have been documented in other intertidal and mangrove systems (Broman et al. 2022; Lobo et al. 2024; Toumi et al. 2024; Wan et al. 2024). In our study, these patterns indicate that environmental gradients influence *Nypa* and benthos in a similar manner and that reductions in *Nypa* biomass and structural complexity may exacerbate the negative effects of salinity on benthic communities by decreasing detrital supply and bioturbation.

The approximately 95% reduction in *Nypa* aboveground biomass (AGB) between the estuarine and coastal zones in Pangkal Babu is comparable in magnitude to the biomass reductions observed along salinity gradients in other mangrove ecosystems. Research conducted in the deltaic systems of the Mekong and Sundarbans has documented a 50–80% decrease in aboveground biomass from oligohaline to polyhaline sites (Dang et al. 2022; Friess et al. 2022). Additionally, peat-dominated mangrove belts in Sumatra and South Borneo exhibit reduced productivity and carbon storage, where sea-level rise and salinity intrusion intensify marine influence (Hapsari et al. 2022; Suello et al. 2022).

Our findings extend these observations by explicitly linking *Nypa* biomass, carbon, and chlorophyll to benthic diversity and abundance along a measured salinity–pH gradient on acidic peat coasts. Similarly, the simplification of benthic assemblages observed at our coastal sites reflects patterns from anthropogenically stressed or high-salinity mangrove flats in the Indian and Atlantic tropics, where macrofaunal richness and functional diversity decline with increasing salinity and disturbance (Lam-Gordillo et al. 2021; Ferreira et al. 2024). The estuarine plots at Pangkal Babu exhibited high *Nypa* biomass and structurally complex benthic communities, whereas the coastal plots displayed low biomass with simplified benthos. This suggests that *Nypa*–benthos coupling is not merely a local phenomenon but may also be representative of other peat-influenced estuaries in Southeast Asia.

From an ecosystem service perspective, the estuarine *Nypa*–benthos mosaics in Pangkal Babu are significant hotspots for aboveground carbon storage and benthic functional diversity. Although wave attenuation and sediment accretion were not measured, our findings align with existing evidence that dense mangrove stands contribute to shoreline protection, detrital processing, and fisheries habitat (Doelle and Puthucherril 2021; Meijer et al. 2021; Hülsen et al. 2023; Ferreira et al. 2024). The substantial biomass and diverse macrofaunal assemblages in the upper estuary likely enhance sediment stability, oxygenation, and carbon burial, whereas the sparser vegetation and simplified fauna in coastal plots suggest a diminished capacity to provide these functions. These results underscore three management priorities for peat-dominated coasts: (i) Conserving estuarine *Nypa* stands with the highest biomass and benthic diversity as core zones for blue carbon storage and biodiversity; (ii) Safeguarding freshwater inflows and hydrological connectivity to buffer upper estuary salinity and maintain low-salinity, strongly acidic conditions that favor high productivity; (iii) Treating *Nypa* stands and associated mudflats as integrated management units in monitoring and conservation programs, recognizing the tight coupling between vegetation structure, benthic ecosystem engineers, and sediment processes. Incorporating *Nypa* habitats into blue carbon accounting frameworks acknowledges their dual role as carbon sinks and biodiversity reservoirs and can support nature-based adaptation strategies for sea-level rise and coastal change (Adame et al. 2024; Lovelock et al. 2024).

Our study had several limitations that warrant consideration when interpreting the results. First, the sampling design employed was purposive and gradient-focused rather than probabilistic, potentially leading to an over-representation of accessible shorelines and structurally intact stands. Nonetheless, the pronounced zone effects on aboveground biomass (AGB) and diversity (partial $\eta^2 \approx 0.755$ for AGB; ≈ 0.635 for H′) indicate that the primary gradients remain robust despite this limitation. Second, all measurements were conducted during a single late wet season campaign (May–June 2025), precluding an assessment of how *Nypa* productivity and benthic assemblages respond to intra-annual variability in salinity, extreme events, or interannual climate anomalies. Consequently, the observed patterns should be regarded as spatial baseline images. Third, our benthic inventory focused on microhabitats characterised by *Nypa*-dominated soft peat-mud and surface-active macrofauna. Gastropods were occasionally observed on the exposed prop roots of adjacent *Rhizophora* and *Avicennia* stands at the plot peripheries, but were absent within the sampled quadrats under dense *Nypa* clusters. Consequently, they are absent from our quantitative dataset and should not be construed as being absent from the broader mangrove mosaic. Fourth, we did not directly measure dissolved oxygen or nutrient concentrations (e.g. dissolved inorganic N and P) in the water column during the study. Therefore, our interpretation primarily relies on salinity and soil pH as proxies for hydrochemical stress. Future research should integrate macrofaunal and vegetation surveys with continuous measurements of dissolved oxygen, nutrients, and sediment geochemistry to elucidate causal mechanisms.

Conclusion, along the estuarine–coastal gradient of an acidic peat coast in eastern Sumatra, both *N. fruticans* productivity and benthic macrofaunal richness peaked in low-salinity, strongly acidic estuarine zones and declined toward more saline, near-neutral coastal sites. Multivariate analyses showed that these patterns were primarily structured by a salinity–pH axis, highlighting the joint role of hydrochemical conditions in shaping vegetation and benthic assemblages. Estuarine *Nypa* belts thus function as key hotspots for aboveground blue carbon and benthic functional diversity. Maintaining freshwater inflows and hydrological connectivity is essential to sustain oligohaline, peat-influenced conditions that support shoreline stability, detrital processing, and fish habitat. Future studies should expand to multi-season monitoring, detailed sediment biogeochemistry, plant physiological metrics, and broader infaunal coverage to clarify how salinity–pH shifts affect vegetation and benthic ecosystem engineers, thereby informing adaptive management of Indonesia's peat-fringed coasts under rising sea levels and salinity intrusion.

ACKNOWLEDGEMENTS

This research was supported by the Indonesia Endowment Fund for Education (*Lembaga Pengelola Dana Pendidikan*/LPDP), Ministry of Finance, Republic of Indonesia. We thank the Department of Environment (*Dinas Lingkungan Hidup*/DLH) of Tanjung Jabung Barat District, Jambi, Indonesia, for permission to conduct research in the Pangkal Babu coastal region from May to June 2025, and appreciate the Pangkal Babu Village community's assistance during sampling. Laboratory analyses were conducted at the Faculty of Science and Technology of Universitas Jambi. We thank the Master's Program in Aquatic Resources Management, Universitas Diponegoro, Semarang, Central Java, Indonesia, for academic guidance. All field activities followed local environmental regulations and ethical standards, with authorization from the DLH, Tanjung Jabung Barat District for May-June 2025, and no protected species were harmed during sampling.

REFERENCES

Abidin Z, Setiawan B, Muhaimin AW, Shinta A. 2021. The role of coastal biodiversity conservation on sustainability and environmental awareness in mangrove ecosystem of southern Malang, Indonesia. Biodiversitas 22 (2): 648-658. DOI: 10.13057/biodiv/d220217.

Adame MF, Kelleway J, Krauss KW, Lovelock CE, Adams JB, Trevathan-Tackett SM, Noe G, Jeffrey L, Ronan M, Zann M, Carnell PE, Iram N, Maher DT, Murdiyarso D, Sasmito S, Tran DB, Dargusch P, Kauffman JB, Brophy L. 2024. All tidal wetlands are blue carbon ecosystems. Bioscience 74 (4): 253-268. DOI: 10.1093/biosci/biae007.

Afonso F, Felix PM, Chainho P, Heumüller JA, De Lima RF, Ribeiro F, Brito AC. 2021. Assessing ecosystem services in mangroves: Insights from São Tomé Island (Central Africa). Front Environ Sci 9: 501673. DOI: 10.3389/fenvs.2021.501673.

Alongi DM. 2020. Global significance of mangrove blue carbon in climate change mitigation. Sci 2 (3): 67. DOI: 10.3390/sci2030067.

Arifanti VB, Sidik F, Mulyanto B, Susilowati A, Wahyuni T, Subarno, Yuniarti N, Yuniarti N, Aminah A, Suita E, Karlina E, Suharti S, Pratiwi, Turjaman M, Hidayat A, Rachmat HH, Imanuddin R, Yeny I, Darwiati W, Sari N, Hakim SS, Slamet WY, Novita N. 2022. Challenges and strategies for sustainable mangrove management in Indonesia: A review. Forests 13: 695. DOI: 10.3390/f13050695.

Arnon DI. 1949. Copper enzymes in isolated chloroplasts. Polyphenoloxidase in Beta vulgaris. Plant Physiol 24 (1): 1-15. DOI: 10.1104/pp.24.1.1.

Basyuni M, Sulistiyono N, Ginting TT et al. 2022. Mangrove biodiversity, conservation and roles for livelihoods in Indonesia. In: Pullaiah DSC, Ashton EC (eds). Mangroves: Biodiversity, Livelihoods and Conservation. Springer, Singapore, DOI: 10.1007/978-981-19-0519-3_16.

Broman E, Izabel-Shen D, Rodríguez-Gijón A, Bonaglia S, Garcia SL, Nascimento FJA. 2022. Microbial functional genes are driven by gradients in sediment stoichiometry, oxygen, and salinity across the Baltic benthic ecosystem. Microbiome 10 (1): 126. DOI: 10.1186/s40168-022-01321-z.

Brown S. 1997. Estimating Biomass and Biomass Change of Tropical Forests: A Primer. FAO Forestry Paper 134. Food and Agriculture Organization of the United Nations, Rome.

Cannicci S, Lee SY, Bravo H, Cantera-Kintz JR, Dahdouh-Guebas F, Fratini S, Fusi M, Jimenez PJ, Nordhaus I, Porri F, Diele K. 2021. A functional analysis reveals extremely low redundancy in global mangrove invertebrate fauna. Proc Natl Acad Sci U S A 118 (32): e2016913118. DOI: 10.1073/pnas.2016913118.

Carpenter KE, Niem VH. 1998. FAO Species Identification Guide for Fishery Purposes: The Living Marine Resources of the Western Central Pacific. Volume 1. Seaweeds, Corals, Bivalves and Gastropods. Food and Agriculture Organization of the United Nations, Rome.

Coppock RL, Lindeque PK, Cole M, Galloway TS, Näkki P, Birgani H, Richards S, Queirós AM. 2021. Benthic fauna contribute to microplastic sequestration in coastal sediments. J Hazard Mater 415: 125583. DOI: 10.1016/j.jhazmat.2021.125583.

Custodio M, Peñaloza R, Chanamé F, Yaranga R, Pantoja R. 2018. Assessment of the aquatic environment quality of high Andean lagoons using multivariate statistical methods in two contrasting climatic periods. J Ecol Eng 19 (6): 24-33. DOI: 10.12911/22998993/92677.

Dang ATN, Reid M, Kumar L. 2022. Assessing potential impacts of sea level rise on mangrove ecosystems in the Mekong Delta, Vietnam. Reg Environ Change 22: 70. DOI: 10.1007/s10113-022-01925-z.

Doelle M, Puthucherril TG. 2021. Nature-based solutions to sea level rise and other climate change impacts on oceanic and coastal environments: A law and policy perspective. Nord J Bot 2023 (1): e03051. DOI: 10.1111/njb.03051.

FAO. 1999. The Living Marine Resources of the Western Central Pacific. FAO Species Identification Guide for Fishery Purposes. FAO, Rome.

Ferreira AC, Ashton EC, Ward RD, Hendy I, Lacerda LD. 2024. Mangrove biodiversity and conservation: Setting key functional groups and risks of climate-induced functional disruption. Diversity 16 (7): 423. DOI: 10.3390/d16070423.

Friess DA, Adame MF, Adams JB, Lovelock CE. 2022. Mangrove forests under climate change in a 2°C world. WIREs Climate Change 13 (4): e792. DOI: 10.1002/wcc.792.

Hapsari KA, Jennerjahn T, Nugroho SH, Yulianto E, Behling H. 2022. Sea level rise and climate change acting as interactive stressors on development and dynamics of tropical peatlands in coastal Sumatra and South Borneo since the Last Glacial Maximum. Glob Chang Biol 28 (10): 3459-3479. DOI: 10.1111/gcb.16131.

Hatje V, Copertino M, Patire VF, Ovando X, Ogbuka J, Johnson BJ, Kennedy H, Masque P, Creed JC. 2023. Vegetated coastal ecosystems in the Southwestern Atlantic Ocean are an unexploited opportunity for climate change mitigation. Commun Earth Environ 4: 160. DOI: 10.1038/s43247-023-00828-z.

Hui TKL, Lo ICN, Wong KKW, Tsang CTT, Tsang LM. 2024. Metagenomic analysis of gut microbiome illuminates the mechanisms and evolution of lignocellulose degradation in mangrove herbivorous crabs. BMC Microbiol 24 (1): 57. DOI: 10.1186/s12866-024-03209-4.

Hülsen S, Mcdonald RI, Chaplin-Kramer R, Bresch DN, Sharp R, Worthington T, Kropf CM. 2023. Global protection from tropical cyclones by coastal ecosystems—past, present, and under climate change. Environ Res Lett 18: 124023. DOI: 10.1088/1748-9326/ad00cd.

Lam-Gordillo O, Baring R, Dittmann S. 2021. Taxonomic and functional patterns of benthic communities in southern temperate tidal flats. Front Mar Sci 8: 723749. DOI: 10.3389/fmars.2021.723749.

Lobo LQ, Izabel-Shen D, Albertsson J, Raymond C, Gunnarsson JS, Broman E, Nascimento FJ. 2024. Salinity and resource availability as drivers of Baltic benthic fungal diversity. Environmental DNA 6 (1): e526. DOI: 10.1002/edn3.526.

Lovelock CE, Bennion V, de Oliveira M, Hagger V, Hill JW, Kwan V, Pearse AL, Rossini RA, Twomey AJ. 2024. Mangrove ecology guiding the use of mangroves as nature-based solutions. J Ecol 112 (11): 2510-2521. DOI: 10.1111/1365-2745.14383.

Mackinney G. 1941. Absorption of light by chlorophyll solutions. J Biol Chem 140 (2): 315-322. DOI: 10.1016/S0021-9258(18)51320-X.

Magurran AE. 2021. Measuring biological diversity. Curr Biol 31 (19): R1174-R1177. DOI: 10.1016/j.cub.2021.07.049.

Meijer KJ, El-Hacen EH, Govers LL, Lavaleye M, Piersma T, Olff H. 2021. Mangrove-mudflat connectivity shapes benthic communities in a tropical intertidal system. Ecol Indic 130: 108030. DOI: 10.1016/j.ecolind.2021.108030.

Murdiyarso D, Donato D, Kauffman JB, Kurnianto S, Stidham M, Kanninen M. 2009. Carbon Storage in Mangrove and Peatland Ecosystems: A Preliminary Account from Plots in Indonesia. Working Paper 48. Center for International Forestry Research (CIFOR), Bogor.

Perri S, Detto M, Porporato A, Molini A. 2023. Salinity-induced limits to mangrove canopy height. Glob Ecol Biogeogr 32 (9): 1561-1574. DOI: 10.1111/geb.13720.

Pielou EC. 1966. The measurement of diversity in different types of biological collections. J Theor Biol 13: 131-144. DOI: 10.1016/0022-5193(66)90013-0.

Qureshi NA, Saher NU. 2024. Burrow morphology of three species of fiddler crab (Uca) along the coast of Pakistan. Belg J Zool 142 (2): 114-126. DOI: 10.26496/bjz.2012.152.

Reed DC, Schmitt RJ, Burd AB, Burkepile DE, Kominoski JS, McGlathery KJ, Miller RJ, Morris JT, Zinnert JC. 2022. Coastal ecosystem responses to climate change: Insights from long-term ecological research. Bioscience 72 (9): 871-888. DOI: 10.1093/biosci/biac006.

Rumondang R, Feliatra F, Warningsih T, Yoswati D. 2024. Sustainable management model and ecosystem services of mangroves based on socio-ecological system on the coast of Batu Bara Regency, Indonesia. Environ Res Commun 6 (3): 035008. DOI: 10.1088/2515-7620/ad2d01.

Shannon CE. 1948. A mathematical theory of communication. Bell Syst Tech J 27: 379-423. DOI: 10.1002/j.1538-7305.1948.tb01338.x.

Simpson EH. 1949. Measurement of diversity. Nature 163: 688. DOI: 10.1038/163688a0.

Suello RH, Hernandez SL, Bouillon S, Belliard J-P, Dominguez-Granda L, Van de Broek M, Rosado Moncayo AM, Ramos Veliz J, Ramirez KP, Govers G, Temmerman S. 2022. Mangrove sediment organic carbon storage and sources in relation to forest age and position along a deltaic salinity gradient. Biogeosciences 19: 1571-1585. DOI: 10.5194/bg-19-1571-2022.

Syafina HA, Hartoko A, Purnomo PW. 2025. Ecological patterns of nipa palm (*Nypa fruticans*) in peatland mangroves of Eastern Sumatra. Intl J Agric Environ Res 11 (5): 1376-1395. DOI: 10.51193/IJAER.2025.11501.

Toumi C, Gauthier O, Grall J, Thiébaut É, Boyé A. 2024. Disentangling the effects of space, time, and environmental and anthropogenic drivers on coastal macrobenthic β diversity in contrasting habitats over 15 years. Sci Total Environ 946: 173919. DOI: 10.1016/j.scitotenv.2024.173919.

Vázquez-Rosas-Landa M, Pérez-Ceballos R, Zaldívar-Jiménez A, Hereira S, Pérez González L, Prieto-Davó A, Celis-Hernández O, Canales-Delgadillo JC. 2025. Impact of seasonal flooding and loss of hydrological connectivity on microbial community dynamics in mangrove sediments in the southern Gulf of Mexico. PeerJ 13: e19371. DOI: 10.7717/peerj.19371.

Wan X, Fang Y, Jiang Y, Lu X, Zhu L, Feng J. 2024. Temperature and nutrients alter the relative importance of stochastic and deterministic processes in the coastal macroinvertebrates biodiversity assembly on long-time scales. Ecol Evol 14 (2): e11062. DOI: 10.1002/ece3.11062.

Wu W, Feng X, Wang N, Shao S, Liu M, Si F, Chen L, Jin C, Xu S, Guo Z, Zhong C, Shi S, He Z. 2024. Genomic analysis of *Nypa fruticans* elucidates its intertidal adaptations and early palm evolution. J Integr Plant Biol 66 (4): 824-843. DOI: 10.1111/jipb.13625.

Xu S, Guo Z, Feng X, Shao S, Yang Y, Li J, Zhong C, He Z, Shi S. 2021. Where whole-genome duplication is most beneficial: Adaptation of mangroves to a wide salinity range between land and sea. Mol Ecol 32 (2): 460-475. DOI: 10.1111/mec.16320.

Yazdian H, Jaafarzadeh N, Zahraie B. 2014. Relationship between benthic macroinvertebrate bio-indices and physicochemical parameters of water: A tool for water resources managers. J Environ Health Sci Eng 12: 30. DOI: 10.1186/2052-336X-12-30.

Yoshikai M, Nakamura T, Suwa R, Sharma S, Rollon R, Yasuoka J, Egawa R, Nadaoka K. 2022. Predicting mangrove forest dynamics across a soil salinity gradient using an individual-based vegetation model linked with plant hydraulics. Biogeosciences 19 (6): 1813-1832. DOI: 10.5194/bg-19-1813-2022.